Supplementary Information Table of Contents

Materials. Dulbecco's Modified Eagle's Medium (DMEM), **P**oly(**m**aleic **a**nhydride-alt-1-**o**ctadecene) (PMAO, Mn=30,000-50,000), ethylenediamine, DMF, tert-butanol and trypsin-EDTA solution were purchased from Sigma-Aldrich (MO, USA). PEG_{2K}-NHS was purchased from JenKem Technology (TX, USA). Dicyandiamide was purchased from TCI America (OR, USA). Fetal bovine serum (FBS) and penicillin-streptomycin solution were purchased from Invitrogen (NY, USA). Antibodies used for flow cytometry were purchased from established vendors such as BioLegend and BD Biosciences. Dicyandiamide was purchased from TCI America Company (PA, USA).

Bulk messenger RNA-seq analysis. RNA-seq was performed by the Health Sciences Sequencing Core at Children's Hospital of Pittsburgh. BALB/c mice (n=3) bearing s.c. CT26 tumors (~200 mm^3) received i.v. injection of FuOXP NPs (10 mg FuOXP/kg) with empty NPs as a control once every five days for three times. Tumors were harvested at 24 h after the last treatment. RNA-seq libraries were sequenced as 75-base paired-end reads at a depth of ~73 to 77 million reads per sample. Reads were mapped to the mouse genome (GRCm38) using STAR Aligner 2.6.1a[1]. Gene expression quantification and differential expression analysis between empty NPs and FuOXP NPs treatment were performed using Cuffdiff of Cufflinks 2.2.1[2]. Volcano plots were generated to show the overall differential expression, where the x axis indicates the $\log_2$(fold change) ($\log_2$FC) between FuOXP NPs and empty NPs and the y axis indicates the corresponding $-\log_{10}$(P value).

Synthesis of PMBOP: **P**oly(**m**aleic **a**nhydride-alt-1-**o**ctadecene) (**PMAO**, Mn=30,000-50,000, compound **1**, 7 g, 20 mmol of repeating units) and dry and degassed DMSO (150 mL) were added into a 250 mL glass bottle equipped with magnetic bar and placed under an atmosphere of

nitrogen. A volume of 6.67 mL ethylenediamine (100 mmol) in 50 mL dry and degassed DMSO solution was then added to the solution. After stirring at 160 °C under nitrogen for 48 hours, the solution was cooled down to room temperature, to which 1 L of HCl solution (2 mol/L) was added. The precipitate was filtered and washed 3 times with water, and then dried under vacuum at 50 °C to obtain **P**oly(**m**aleimideethylamine-alt-1-**o**ctadecene) polymer (**PMO**, compound **2)**. Then, 392 mg of compound **2** (1 mmol of repeating units), 200 mg of PEG_{2K}-NHS (0.1 mmol), 10 mL of dry DMSO and 1 mL TEA (triethylamine) were added into a 50 mL bottle equipped with magnetic bar. The solution was allowed to stir for 48 hours at room temperature. After the reaction, the solution was transferred to dialysis bag (MWCO 12,000-14,000) and dialyzed against water for 24 hours. After dialysis, the solution was filtered by P5 filter paper and lyophilized to obtain PEG-conjugated PMAO polymer with a yield of about 10-20%. PEG-conjugated PMAO polymer (100 mg) and dicyandiamide (840 mg, 10 mmol) were then dissolved in 10 mL of *tert*-BuOH and refluxed with stirring for 12 hours. After the reaction, the solution was transferred to a dialysis bag (MWCO 12,000-14,000) and dialyzed for 24 hours against water. After lyophilization, the **P**oly(**m**aleimideethyl**b**iscarboximidamide-alt-1-**o**ctadecene)-Poly(maleimideethyl**p**olyethylene-glycol-alt-1-octadecene) (**PMBOP**, compound **3**) was obtained with a yield of ~98%.

Cryo-electron microscopy: Samples were first checked with negative stain electron microscopy by applying 3 µL to a freshly glow-discharged continuous carbon on a copper grid and staining with a 1% uranyl acetate solution. Grids were inserted into a Thermofisher TF20 electron microscope (Thermofisher Scientific, MA, USA) equipped with a field emission gun and imaged on a TVIPS XF416 CMOS camera (TVIPS GmbH, Gauting, Germany) to visualize nanoparticle uniformity and concentration. Cryo-grids were prepared by pipetting 3µL of sample on a Protochips C-flat CF-2/1-3CU-T grid (Protochips, NC, USA) that had been glow discharged at 25 mA for 30 s using an Emitech KX100 glow discharger. Grids were mounted in a Thermofisher

Vitrobot Mk 4 with relative humidity of 95%, blotted for 3 s with a force setting of 4, and plunged into a 40/60 mixture of liquid ethane/propane[3] that was cooled by a bath of liquid nitrogen. Grids were transferred onto a Gatan 910 three-grid cryoholder (Gatan, Inc., CA, USA) and into the TF20 microscope maintaining a temperature no higher than -175 °C throughout. The microscope was operated at 200 kV and contrast was enhanced with a 100 µm objective aperture. Cryo-electron micrographs were collected at a nominal 62,000x magnification on the TVIPS XF416 CMOS camera with a post-column magnification of 1.3x corresponding to a calibrated pixel size of 1.8 Ångstroms at the sample. Low dose methods were used to avoid electron beam damage and images were acquired with TVIPS *Emplified* software using movie mode for drift correction. Exposures included 10 frames at 0.15 s each for a total exposure of 1.5 s, and a total dose of approximately 10 electrons per square Ångstrom.

***In vitro* drug release**: The release of FuOXP from FuOXP-loaded PMBOP-CP NPs with or without siRNA complexation was examined using a dialysis method. Briefly, 200 µL of FuOXP-loaded PMBOP-CP and FuOXP/siXkr8-coloaded PMBOP-CP NPs containing 200 µg of FuOXP and 2 mg of PMBOP were placed in a dialysis bag (MWCO 3.5 kDa) containing 5 mL 0.1 M PBS solution or mouse serum, respectively, and immersed into 40 mL of 0.1 M PBS solution containing 0.5% (w/v) Tween 80. The experiment was performed in an incubation shaker at 37ºC at 100 RPM. At selected time intervals, 10 µL solution in the dialysis bag and 1 mL medium outside the dialysis bag were withdrawn while same amount of fresh dialysis solution was added for replenishment. The concentration of FuOXP was examined by HPLC.

Microscopic study of tumor distribution of NPs. For *in vivo* tumor biodistribution study, CT26 tumor bearing mice (~300 mm^3) were i.v. injected with Cy5.5-siRNA-loaded NPs. The mice were

sacrificed at 24 h post injection. Tumor frozen sections were prepared and fixed with acetone at 4°C for 5 min. Cytoskeleton was stained with AF488-Phalloidin (0.33 μM) (Cell Signaling Technology, MA, USA) at room temperature for 15 min and cell nuclei were stained with Hoechst 33324 (1 μg/mL) (ThermoFisher Scientific, MA, USA) at room temperature for 15 min. Tissue sections were then washed with cold DPBS three times before observation under a confocal laser scanning microscope (CLSM, FluoView 1000, Olympus, Japan).

***In vitro* gene knockdown**: CT26-Luc cells, a CT26 subline stably expressing luciferase were seeded in 24-well plates in antibiotic-free DMEM/FBS. After 24 h, cells were washed with DPBS and incubated for 1 h in DMEM containing various endocytosis pathway inhibitors (**Suppl Table 2**), respectively. Cells were then treated with luciferase-siRNA (siLuc)-loaded PMBOP-CP NPs at a dose of 100 nM siRNA. Cells were washed at 4 h post-transfection with DPBS to remove any extracellular siRNAs and replaced with DMEM/FBS. At 24 h post-transfection, cells were collected and subjected to luciferase assay.

***In vivo* gene knockdown**: MC38-Luc cells were s.c. inoculated into the right lower abdomen of C57BL/6 mice. SiLuc or siCT-loaded PMBOP-CP NPs were injected into MC38-Luc tumor-bearing mice at a dose of 2 mg siRNA/kg. The efficiency of gene knockdown was measured three times by whole-body bioluminescence imaging on the next day following the 1st, 2^{nd,} and 3rd injection on day 10, 15 and 20 post tumor inoculation, respectively. Mice were anesthetized for the first two imaging and euthanized for the final imaging.

In a separate experiment, gene knockdown in liver and tumor by PMBOP-CP NPs was compared to a LNPs (lipid nanoparticles) formulation (cholesterol, DLin-MC3-DMA, DSPC, and PEG_{2000}-

DMG in a 38.5: 50: 10: 1.5 ratio, m/m) used for Onpattro[4]. LNPs co-loaded with siLuc and Factor VII siRNA (siFVII) (1: 1, w/w) were prepared by a microfluidics method using NanoAssemblr Ignite (Precision Nanosystems, BC, Canada)[5]. PMBOP-CP NPs co-loaded with the two siRNAs were also prepared. Groups of 3 BALB/c mice bearing CT26-Luc tumors (s.c., ~300 mm^3) received tail vein injection of PMBOP-CP NPs or LNPs at a total siRNA dose of 2 mg/kg once every 3 days for 3 times. Two days after the last injection, mice were sacrificed and blood samples were collected. The level of Factor VII activity in plasma was analyzed using a Biophen FVII assay kit (Aniara Corporation, OH, USA). Tumors were also collected, homogenized and the level of luciferase activity was analyzed using Pierce™ Firefly Luciferase Glow Assay Kit (ThermoFisher Scientific, MA, USA).

CT26 subline with stable mXkr8 knockdown: A set of 3 SMARTvector Mouse Xkr8 Lentiviral mCMV-TurboGFP shRNAs and a SMARTvector control Lentiviral mCMV-TurboGFP shRNA were purchased from Horizon Discovery Biosciences (Cambridge, UK). CT26 cells were transduced with each lentiviral particle and polybrene at an optimal condition and predetermined 10 MOI in 6-well plates. Cells were incubated for 24 h before sorting with TurboGFP to harvest $CT26^{SMART\ mXkr8-/-}$ and $CT26^{SMART}$.

For characterization of cell proliferation in culture, $CT26^{SMART\ mXkr8-/-}$, $CT26^{SMART}$ and $CT26^{WT}$ cells were seeded in 48-well plates at a density of 2 x 10^3 cells/well, respectively and incubated at 37 °C. Cell proliferation was examined by MTT assay at day 1, 2, 3, and 4, respectively.

To examine tumor growth *in vivo*, $CT26^{SMART\ mXkr8-/-}$, $CT26^{SMART}$ and $CT26^{WT}$ were s.c. inoculated into the right lower abdomen of BALB/c mice and the sizes of tumors were monitored every 2

142 days. Tumor volume was calculated by the following formula: tumor volume = 0.5 × length ×
143 width^2.

144

145 For *in vitro* phagocytosis assay, CT26$^{SMART\ mXkr8-/-}$, CT26^{SMART} and CT26^{WT} (target cells) were
146 stained with 5 μM CFSE (ThermoFisher Scientific, MA, USA) and seeded at 2.5 x 10^5 cells/well in
147 uncoated 24-well suspension tissue culture plates. Macrophages isolated from mouse peritoneal
148 cavity were seeded in adherent 24-well plates. Target cells were treated with DMSO or FuOXP
149 for 24 h and then added to macrophages (1: 1 ratio) for co-incubation. Cells were cocultured at
150 37 °C for 1 h, after which the cells were detached from the plates, washed, and stained with
151 macrophage-specific anti-F4/80 antibody for flow analysis[6].

152

153 **Toxicity**: Body weights of mice were followed once every 2 days throughout the *in vivo* therapy
154 study. After completing the experiment, blood samples were collected and ALT and AST were
155 measured by ALT/SGPT or AST/SGOT liqui-UV assay kit following manufacturer's protocols[7].
156 Tumors and major organs including heart, liver, spleen, lung, and kidney were excised and fixed
157 in PBS containing 10% formaldehyde, followed by embedment in paraffin. The paraffin embedded
158 samples were sectioned into slices at 4 μm using an HM 325 Rotary Microtome. The tissue slices
159 were then subjected to H&E staining for histopathological examination under a Zeiss Axiostar
160 plus Microscope (PA, USA).

161

162 In a separate experiment, naive mice (n = 3) received tail vein injection of siRNA-loaded PMBOP-
163 CP NPs or siRNA complexed with DOTAP liposomes (N/P: 10/1) at a siRNA dose of 1 mg/kg.
164 Two h later, blood was collected from the eye socket and the serum cytokine levels (TNF-α and
165 IL-6) were determined with mouse cytokine assay kits.

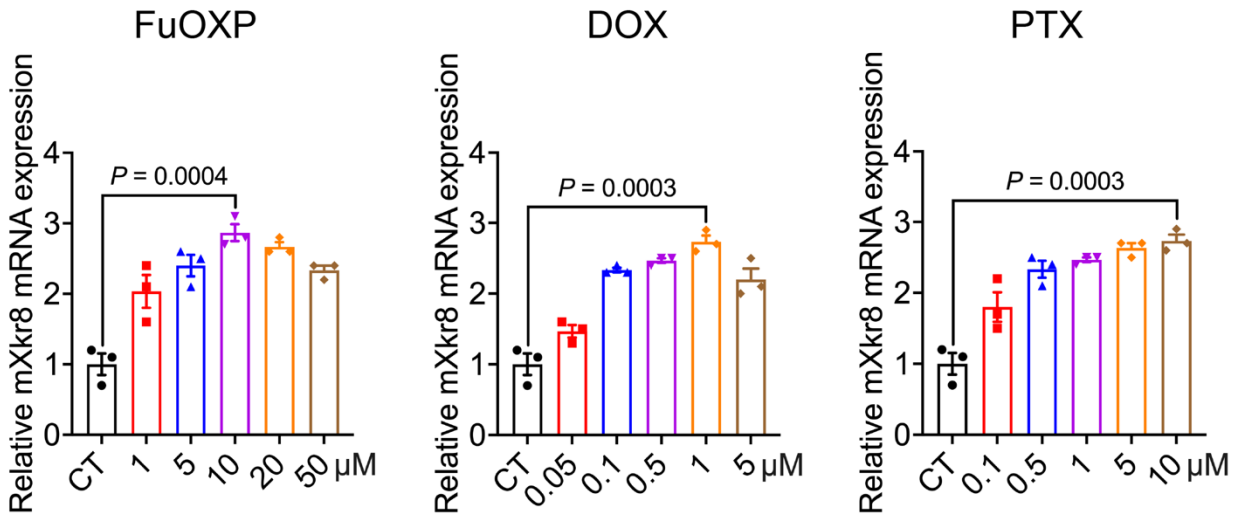

Suppl Fig. 1. Xkr8 induction by different chemotherapy drugs. CT26 tumor cells were treated with various concentrations of FuOXP, DOX or PTX and the expression levels of Xkr8 mRNA were examined 24 h later via qRT-PCR. Data are presented as mean ± SEM (N= 3 replicates) and representative of 2 independent experiments. Statistical analysis was performed by one-way analysis of variance (ANOVA) with Tukey post hoc test for comparison.

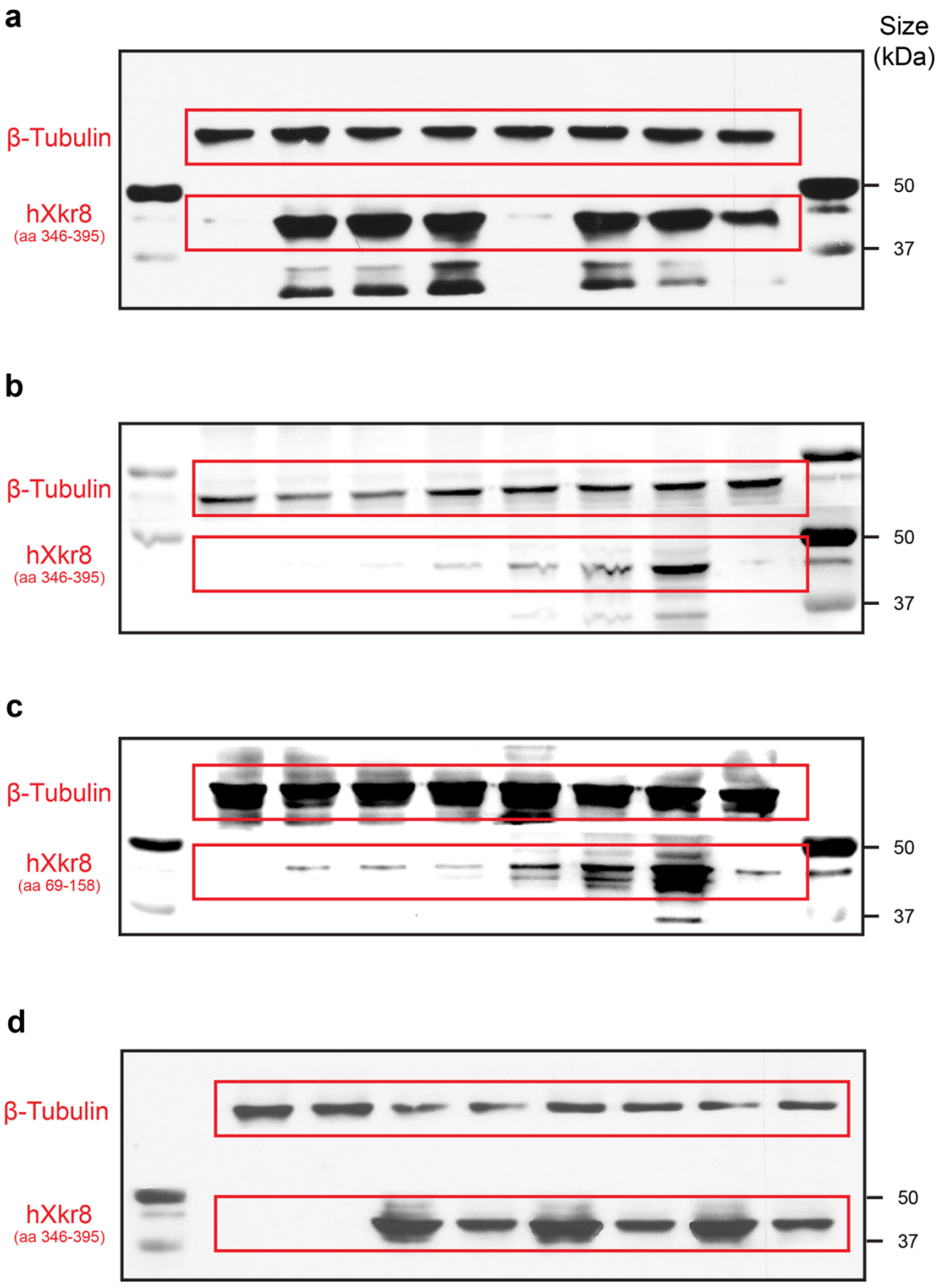

Suppl Fig. 2. Representative Western blots with ladders for Fig. 1d (a), Fig. 1f (b), Fig. 1h (c), and Fig. 1o (d).

Scheme 1

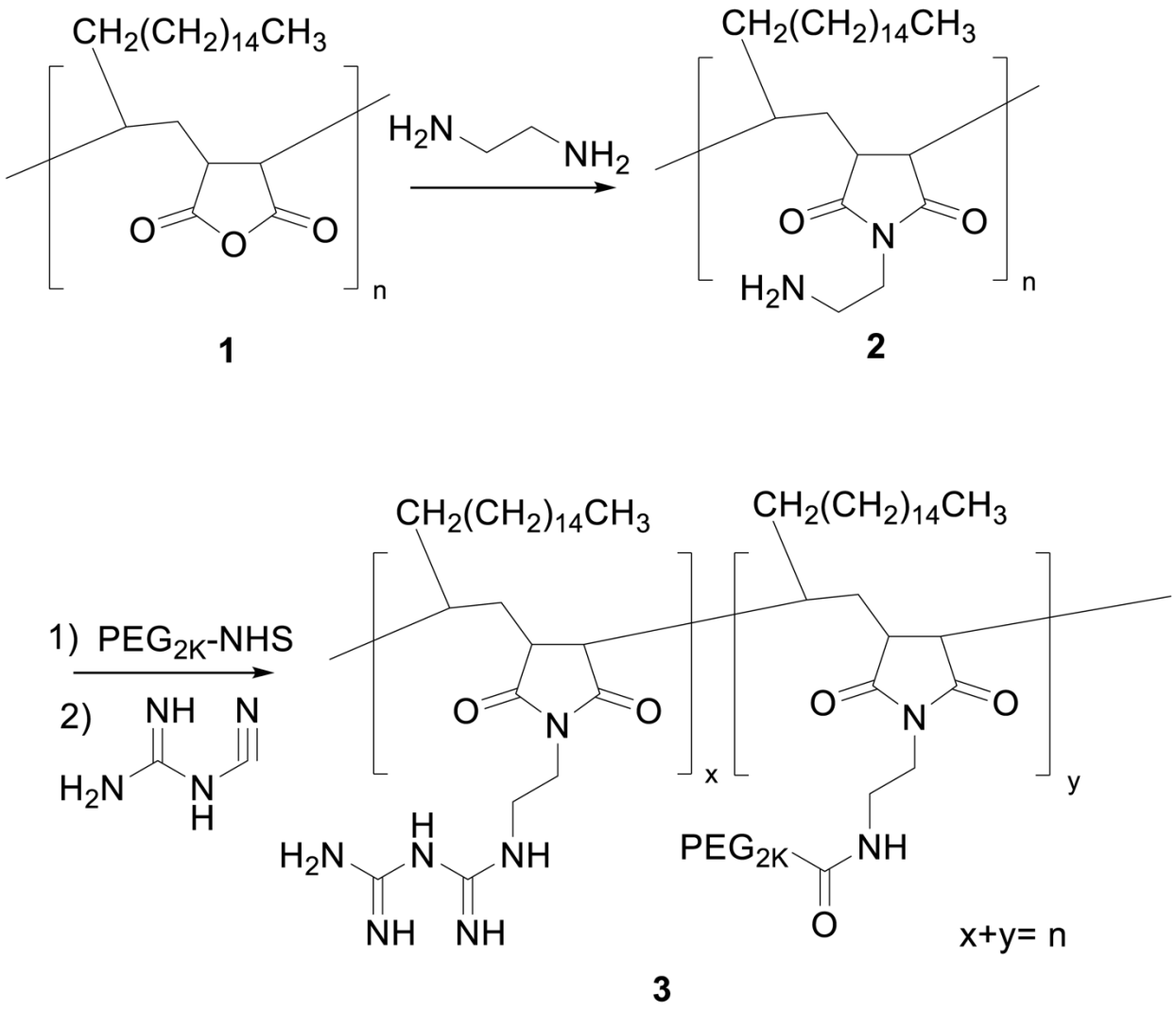

176

177 **Suppl Fig. 3. Synthesis scheme of PMBOP polymer.**

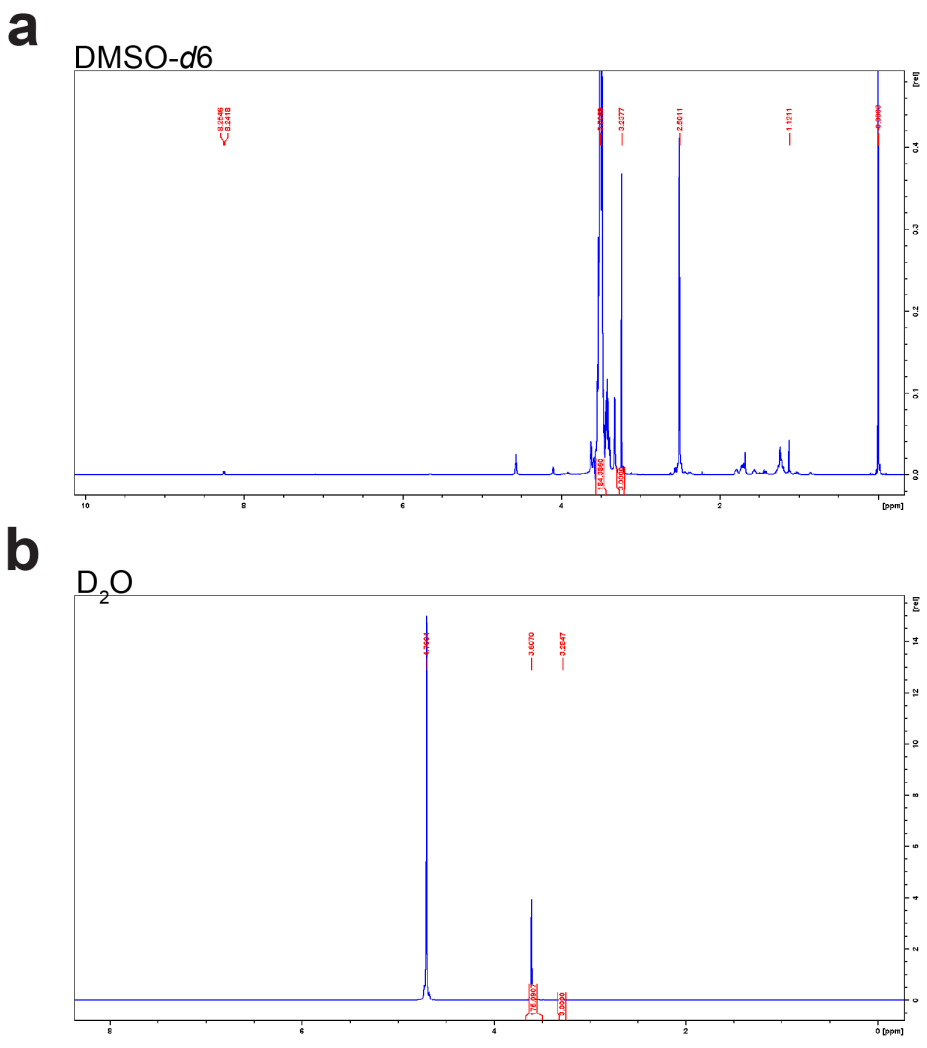

Suppl Fig. 4. ^{1}H nuclear magnetic resonance (NMR) spectra of PMBOP polymer in DMSO-*d*6 (a), and in D_2O (b).

a

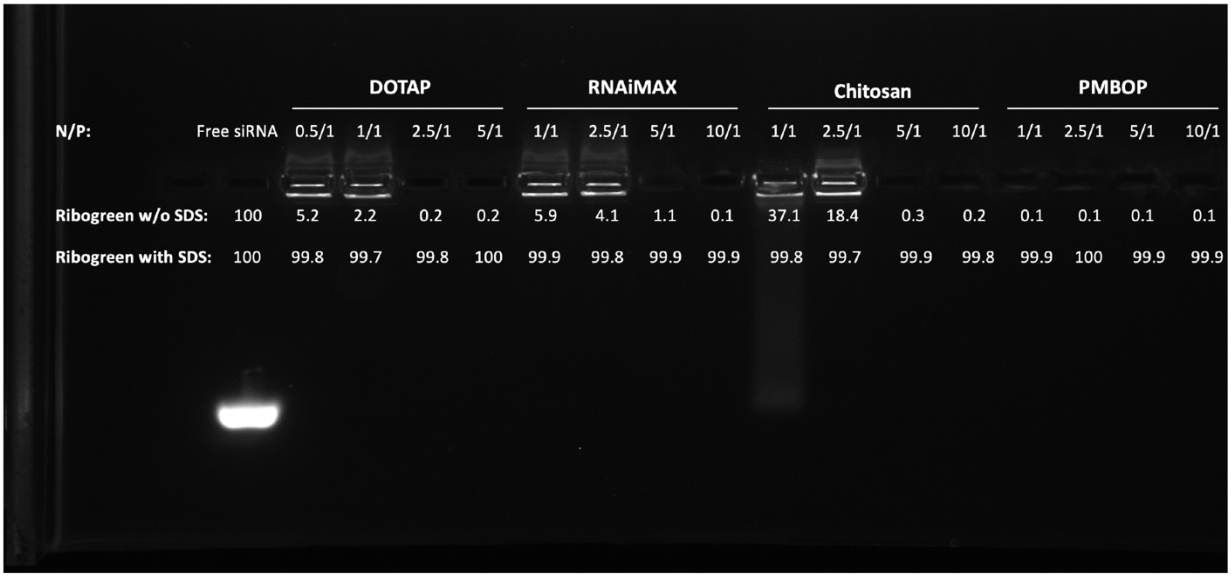

b

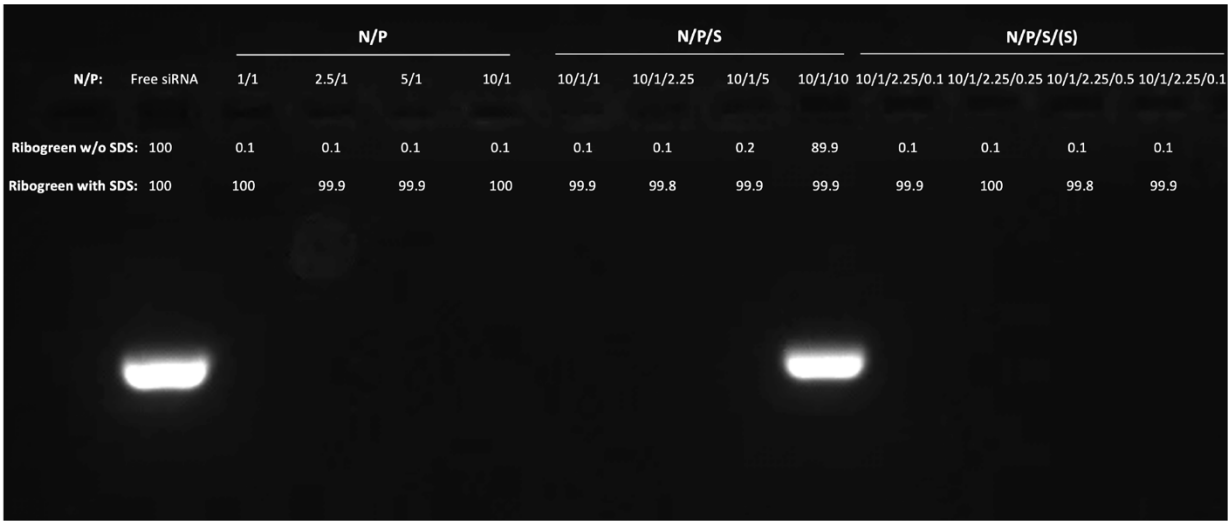

Suppl Fig. 5. Gel retardation assay of various siRNA NPs. a: Gel electrophoresis of siRNA complexed with DOTAP liposome, Lipofectamine RNAiMAX, chitosan polymer or PMBOP at various N/P ratios, showing formation of more compact complex for PMBOP/siRNA. **b**: Gel electrophoresis of PMBOP/siRNA complexes at various N/P ratios, and PMBOP/siRNA complexes (N/P, 10/1) coated with various amounts of CS and PEG-CS. Shown are representative data from 2 independent experiments.

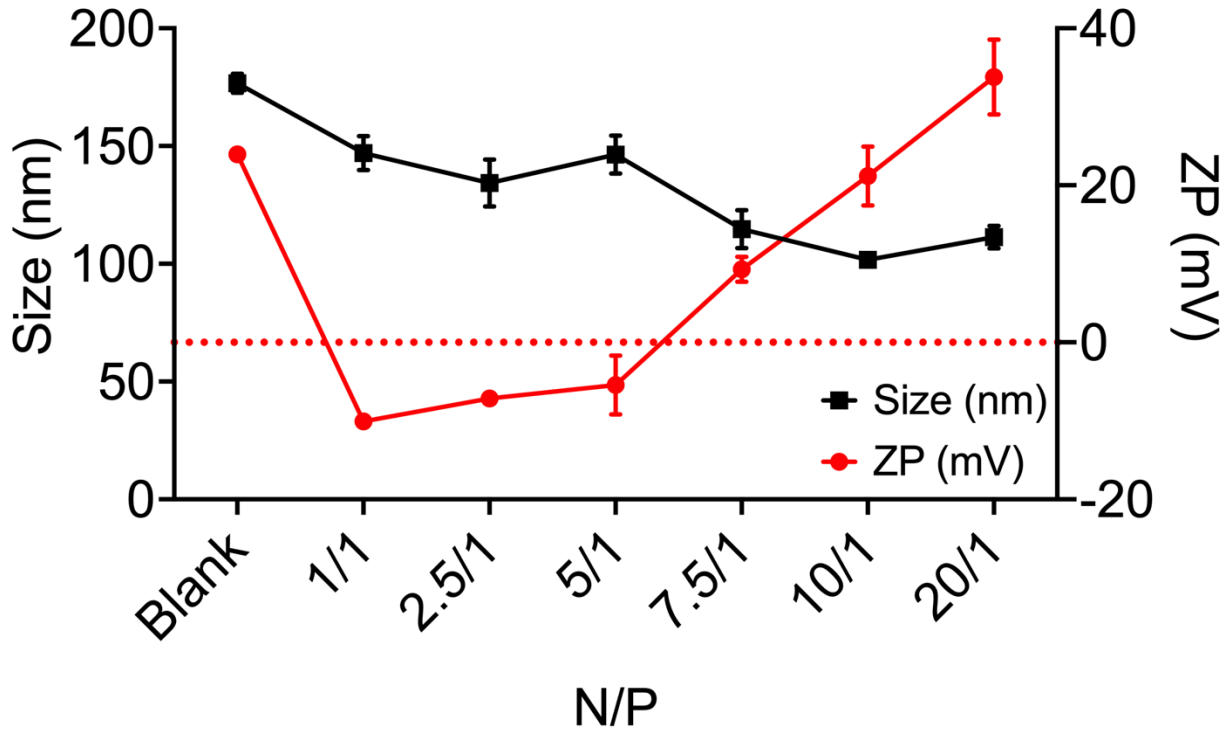

188

189 **Suppl Fig. 6. Sizes and zeta potentials of PMBOP/siRNA complexes at various N/P**

190 **ratios.** Data are presented as mean ± SEM (N=3 replicates) and representative of 3

191 independent experiments

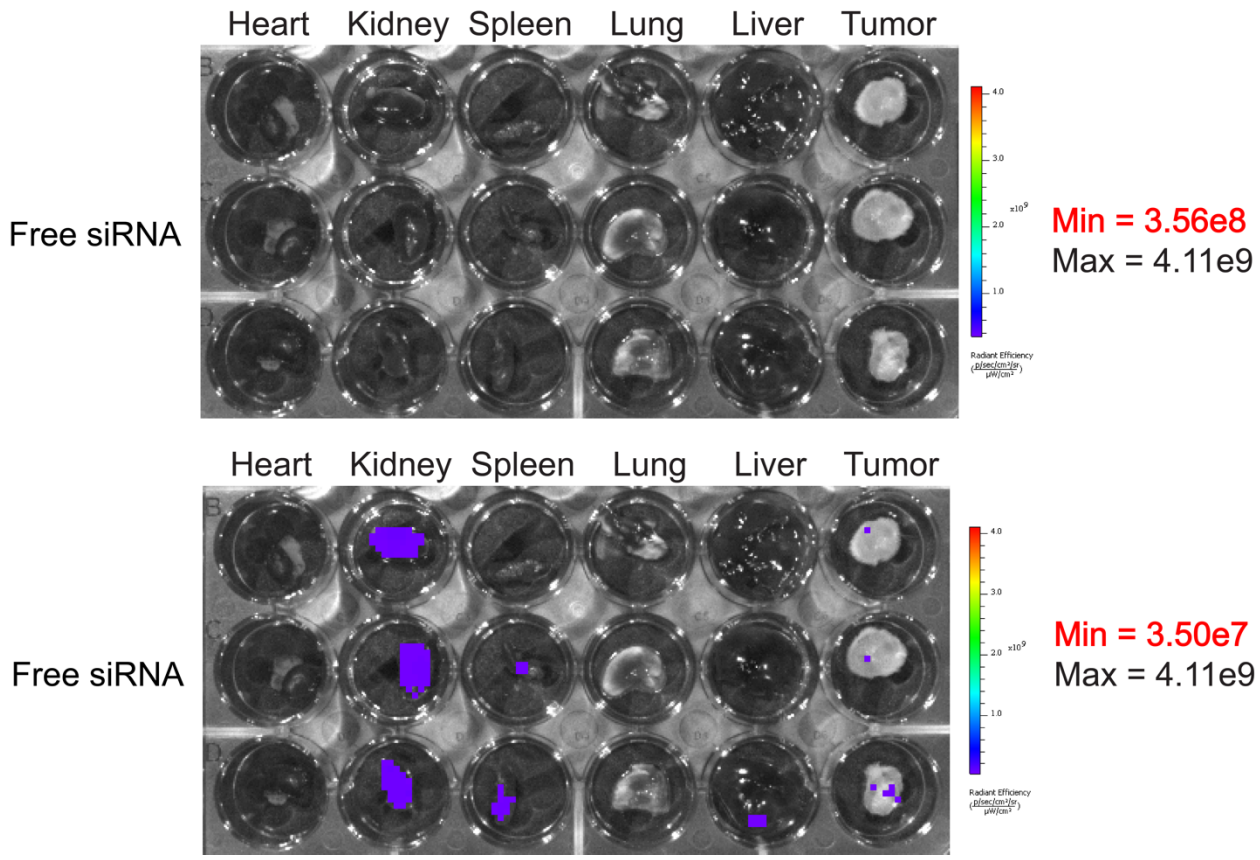

192

193 **Suppl Fig. 7. *Ex vivo* imaging of tumors (CT26) and major organs at 24 h following**

194 **i.v. administration of free Cy5.5-siRNA using two different color scales. Mice were**

195 **treated as detailed in Fig. 3b.**

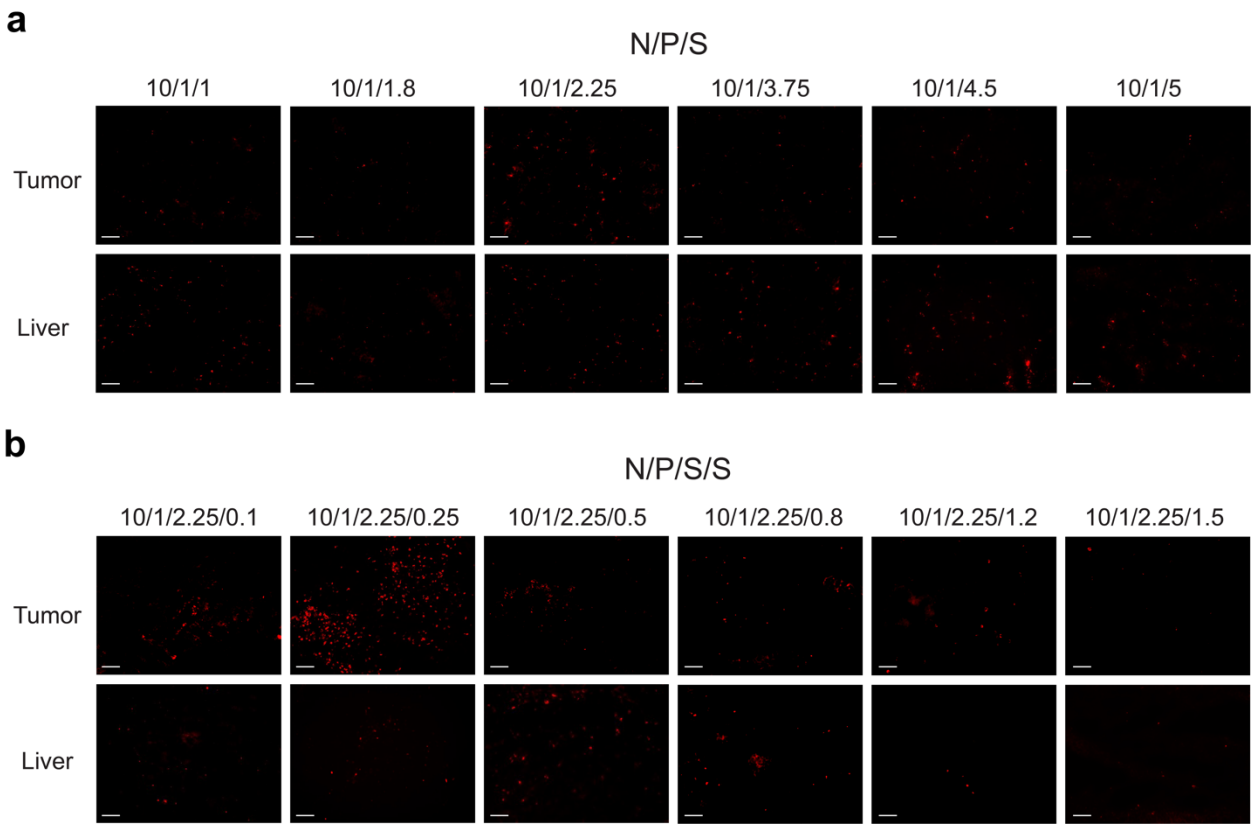

Suppl Fig. 8. Characterizations of PMBOP NPs for *in vivo* delivery of siRNA to tumors. a: Cy5.5-siRNA-loaded PMBOP NPs with a N/P ratio of 10/1 were coated with CS at an N/P/S (CS) ratio from 10/1/1 to 10/1/5, respectively. Tumor and liver sections were prepared at 24 h following i.v. administration of the NPs and examined under a fluorescence microscope. **b**: Cy5.5-siRNA-loaded PMBOP-C NPs with an N/P/S (CS) ratio of 10/1/2.25 were further coated with PEG-CS with the CS/PEG-CS ratios ranging from 2.25/0.1 to 2.25/1.5, respectively. The distribution of Cy5.5-siRNA in tumor and liver sections was then similarly examined. Scale bar, 30 μm. Shown are representative images from 2 batches of tumor samples.

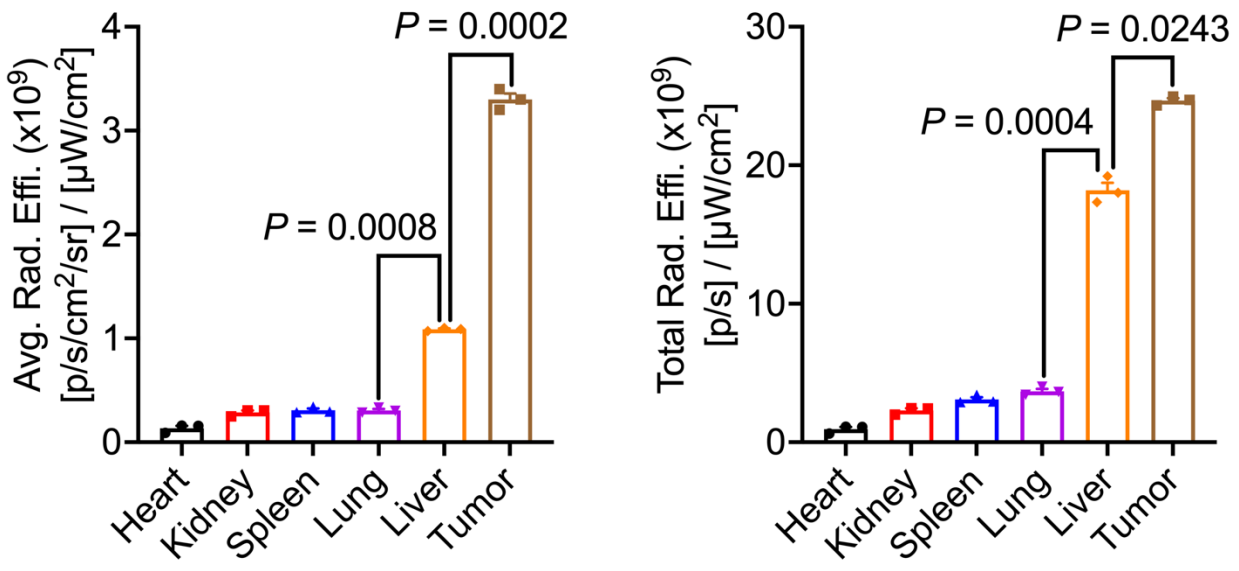

206

207 **Suppl Fig. 9. Quantification of average and total radiance efficiency of fluorescence**

208 **intensity (Cy5.5-siXkr8) in tumor and major organs in Fig. 3d.** Data are presented as

209 mean ± SEM (N= 3 mice per group) and representative of 2 independent experiments.

210 Statistical analysis was performed by one-way analysis of variance (ANOVA) with Tukey

211 post hoc test for comparison.

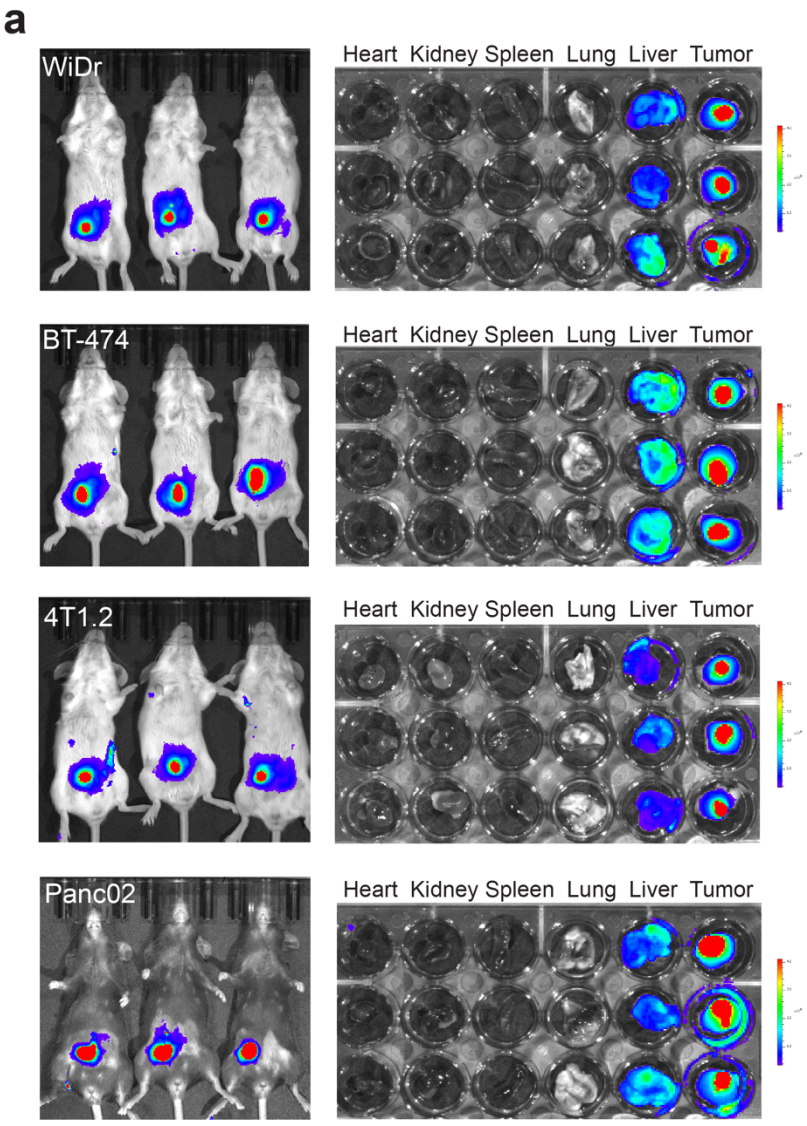
a
WiDr
Heart Kidney Spleen Lung Liver Tumor
BT-474
Heart Kidney Spleen Lung Liver Tumor
4T1.2
Heart Kidney Spleen Lung Liver Tumor
Panc02
Heart Kidney Spleen Lung Liver Tumor
b
P = 0.7321
P = 0.785
CT
WiDr
BT474
4T1.2
Panc02
Avg. Rad. Effi. (x10^9) [p/s/cm^2/sr] / [μW/cm^2]
4.0
3.5
3.0
2.5
2.0
1.5
1.0
0.5
0.0
Tumor
Liver

212

Suppl Fig. 10. Comparison of *in vivo* tumor targeting efficiency of PMBOP-CP NPs among different tumor models. **a**: NIRF whole body and *ex vivo* imaging of tumors and major organs of various tumor-bearing mice at 24 h following i.v. administration of Cy5.5-siRNA-loaded PMBOP-CP NPs. **b**: Fluorescence (Cy5.5-siRNA) intensity at tumors and livers of different tumor-bearing mice at 24 h following i.v. administration of Cy5.5-siRNA-loaded PMBOP-CP NPs. Data are presented as mean ± SEM (N= 3 mice per group) and representative of 2 independent experiments. Statistical analysis was performed by one-way analysis of variance (ANOVA) with Tukey post hoc test for comparison.

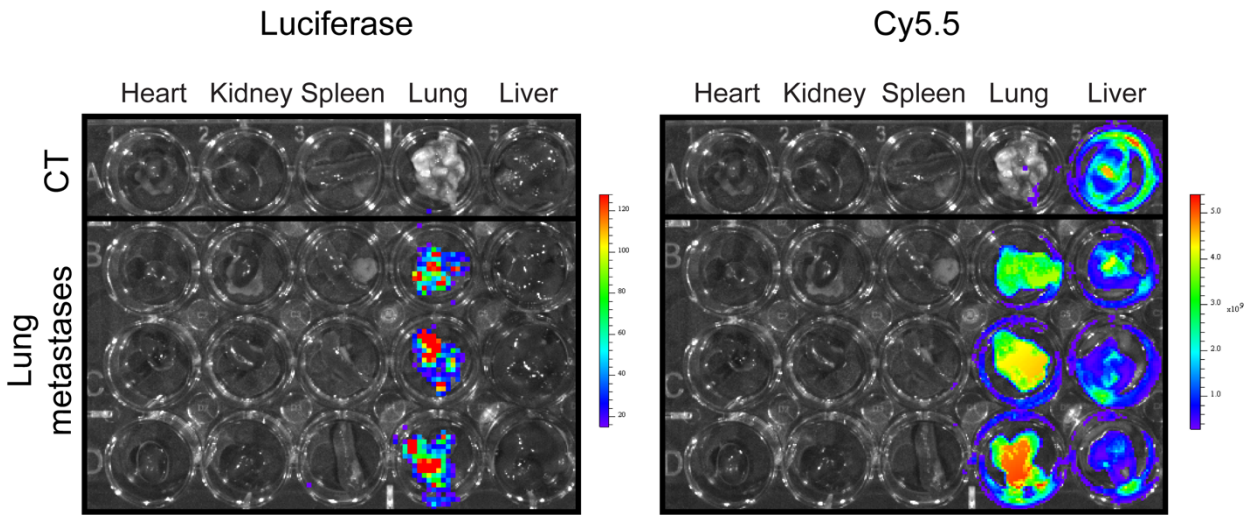

Suppl Fig. 11. *Ex vivo* imaging of metastatic tumors in the lung, and other major organs at 24 h following i.v. administration of Cy5.5-siRNA-loaded PMBOP-CP NPs. Lung metastatic tumor model was established via i.v. injection of CT26-luc cells (5 x 10^5 cells/mouse) and imaging was conducted at 18 days following tumor cell inoculation. Shown are representative images from 2 independent experiments (N=3).

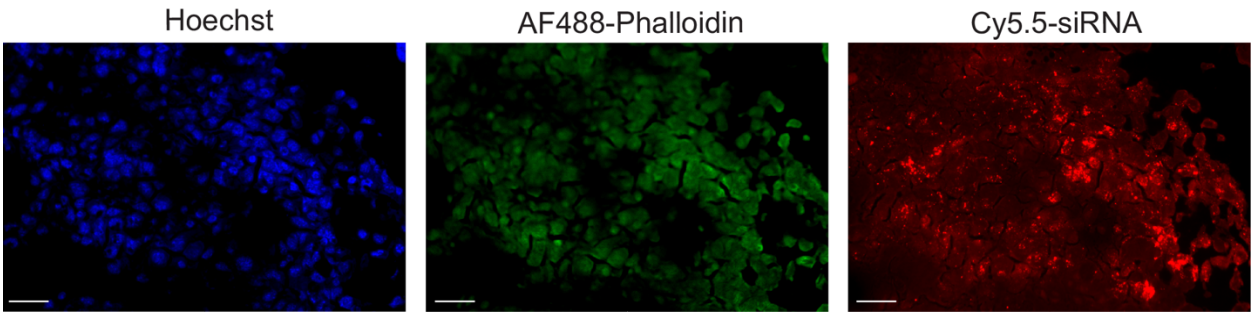

Suppl Fig. 12. *In vivo* delivery of Cy5.5-siRNA to tumors via PMBOP-CP NPs. Confocal laser scanning microscope images of tumor (s.c. CT26) sections at 20x magnification were taken at 24 h following i.v. administration of Cy5.5-siRNA-loaded PMBOP-CP NPs. Cell nuclei were stained with Hoechst and cytoskeleton was stained by AF488-Phalloidin. Scale bar, 30 μm. Shown are representative images from 2 tumor tissues.

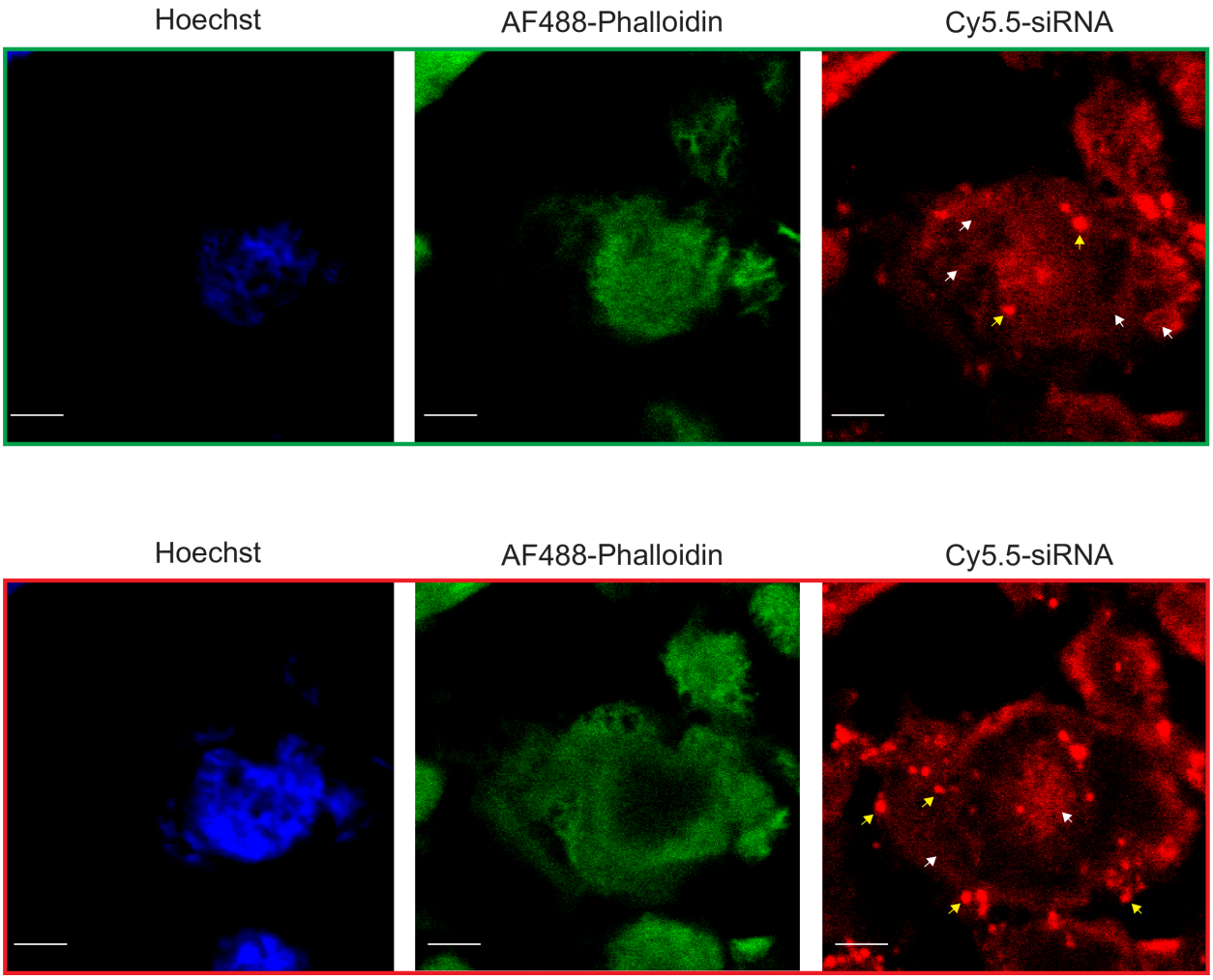

Suppl Fig. 13. *In vivo* delivery of Cy5.5-siRNA to tumors via PMBOP-CP NPs. Confocal laser scanning microscope images of tumor (s.c. CT26) sections at 600x magnification in different layers were taken at 24 h following i.v. administration of Cy5.5-siRNA-loaded PMBOP-CP NPs. Cell nuclei were stained with Hoechst and cytoskeleton was stained by AF488-Phalloidin. Upper panels: 0.1 μm layer from the first scan; Lower panels: 0.5 μm layer from the first scan. Scale bar, 1 μm. Shown are representative images from 2 tumor tissues.

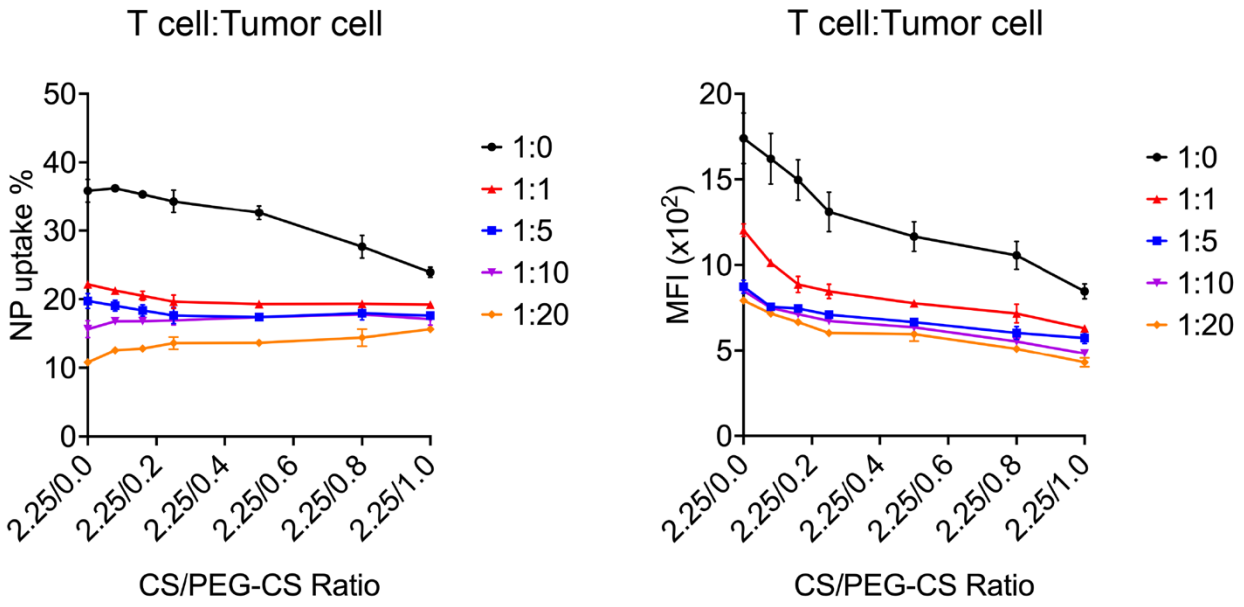

Suppl Fig. 14. The uptake of NPs by T_a in the presence of tumor cells at different T_a/tumor cell ratios. T_a and CT26 were mixed at different ratios and treated with Cy5.5-siRNA-loaded PMBOP-CP NPs coated with various amounts of CS and PEG-CS. Four (4) h later, cellular uptake of Cy5.5-siRNA was examined by flow. Results were expressed as the percentage of $Cy5.5^+$ cells and mean fluorescence intensity (MFI) per cell, respectively. Data are presented as mean ± SEM (N= 3 replicates) and representative of 2 independent experiments.

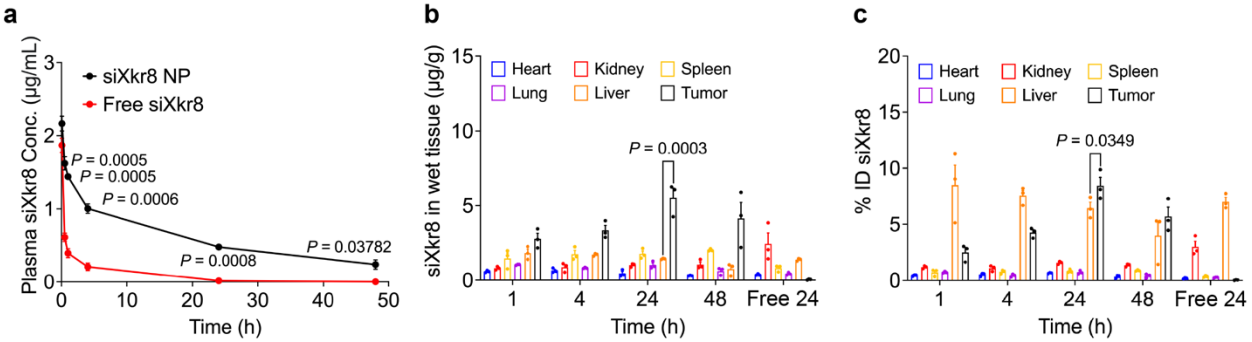
a
Plasma siXkr8 Conc. (μg/mL)
siXkr8 NP
Free siXkr8
P = 0.0005
P = 0.0005
P = 0.0006
P = 0.0008
P = 0.03782
Time (h)
b
siXkr8 in wet tissue (μg/g)
Heart
Kidney
Spleen
Lung
Liver
Tumor
P = 0.0003
Time (h)
c
% ID siXkr8
Heart
Kidney
Spleen
Lung
Liver
Tumor
P = 0.0349
Time (h)

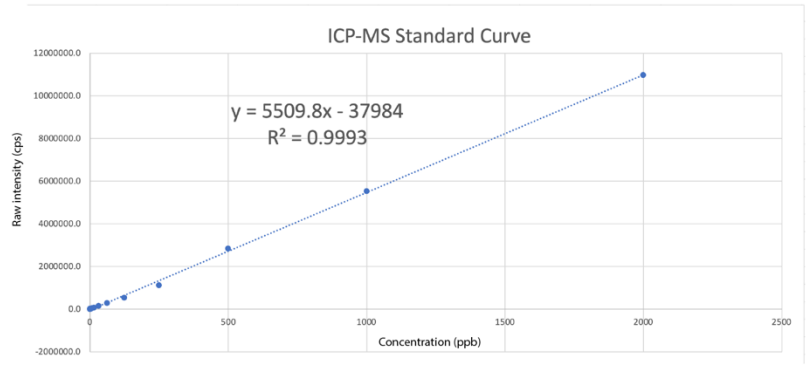
d
ICP-MS Standard Curve
y = 5509.8x - 37984
R² = 0.9993
Raw intensity (cps)
Concentration (ppb)

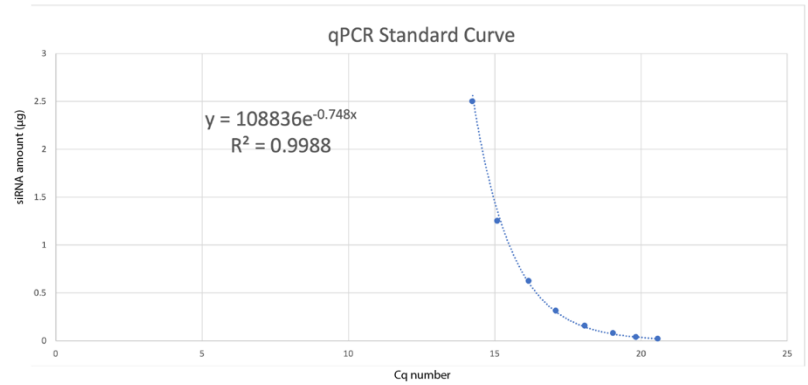
e
qPCR Standard Curve
y = 108836e-0.748x
R² = 0.9988
siRNA amount (μg)
Cq number

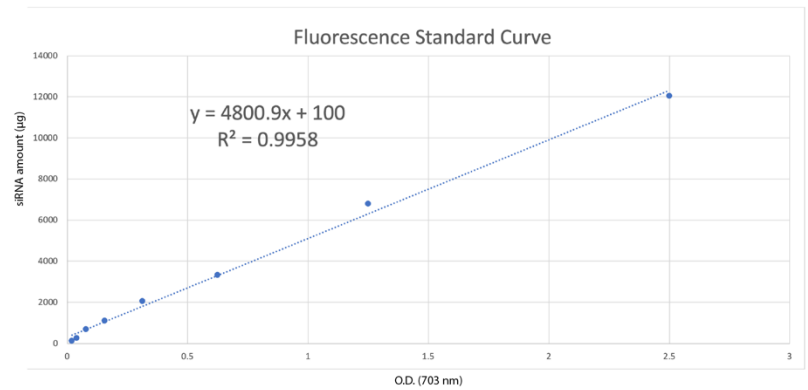
f
Fluorescence Standard Curve
y = 4800.9x + 100
R² = 0.9958
siRNA amount (μg)
O.D. (703 nm)

266

Suppl Fig. 15. *In vivo* PK and tissue distribution of siXkr8 following i.v. administration of FuOXP/Cy5.5-siXkr8 NPs. a: Fluorescence intensity of Cy5.5-siXkr8 in plasma of BALB/c mice bearing CT26 tumors at different times following tail vein injection of free FuOXP/Cy5.5-siXkr8 (in Cremophor EL) and FuOXP/Cy5.5-siXkr8 NPs, respectively. The dose of FuOXP was 5 mg/kg and the siRNA dose was 1 mg/kg. Data are presented as mean ± SEM (N= 3 mice per group) and representative of 2 independent experiments. **b** & **c**: Biodistribution of Cy5.5-siXkr8 in different organs of CT26 tumor-bearing BALB/c mice at different times following tail vein injection of free FuOXP/Cy5.5-siXkr8 and FuOXP/Cy5.5-siXkr8 NPs, respectively. Results were expressed as concentration of siXkr8 in wet tissue (**b**) and % of injected dose of siXkr8 (ID) (**c**), respectively. Data are presented as mean ± SEM (N= 3 mice per group) and representative of 2 independent experiments. **d** & **e**: Standard curves and equations for ICP-MS analysis (**d**), qPCR (**e**), and fluorescence measurement (**f**). Statistical analysis was performed by two-tailed Student's *t*-test for comparison in **a** and one-way analysis of variance (ANOVA) with Tukey post hoc test for comparison in **b** and **c.** FuOXP is capable of forming complex with siRNA in Cremophor EL and protects siRNA, which is attributed to relatively higher amounts of siRNA in liver in comparison to minimal Cy5.5-siRNA signal in liver following i.v. injection of free Cy5.5-siRNA (**Suppl. Fig. 7**).

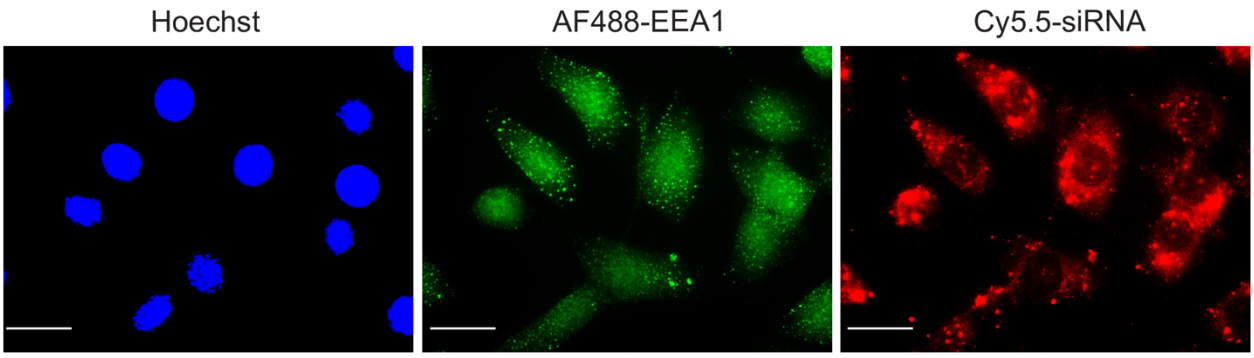

Suppl Fig. 16. *In vitro* cellular uptake of Cy5.5 siRNA-loaded NPs. Cultured CT26 tumors cells were treated with Cy5.5 siRNA-loaded PMBOP-CP NPs and fluorescence microscopic images were taken 2 h later. Nucleus was stained with Hoechst and endosome was stained with AF488 EEA1 antibody. Scale bar, 10 μm. Shown are the representative images from 3 independent experiments.

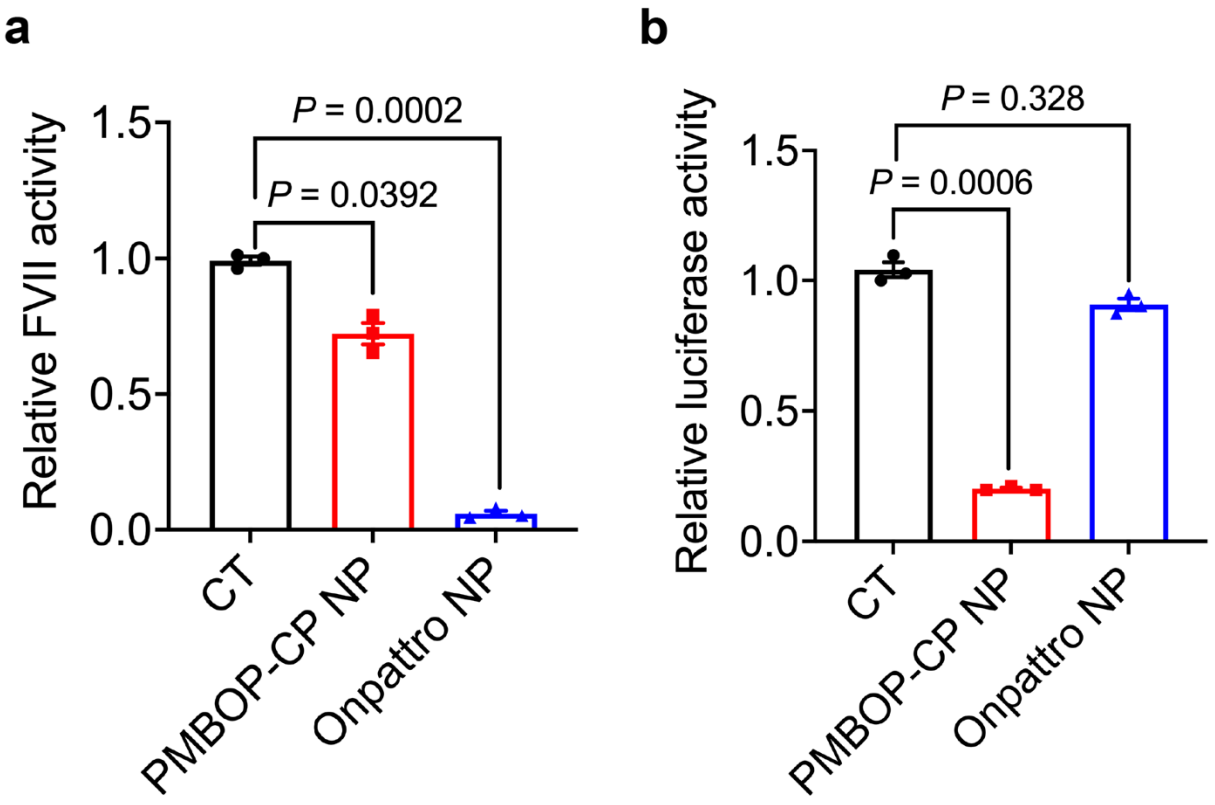

297

298 **Suppl Fig. 17. *In vivo* knockdown of FVII and luciferase.** Groups of 3 BALB/c mice
299 bearing CT26-luc tumors received tail vein injection of PMBOP-CP NPs or Onpattro NPs
300 co-loaded with siFVII and siLuc (1: 1, w/w) at a total siRNA dose of 2 mg/kg once every
301 3 days for 3 times. FVII activity in plasma (**a**) and luciferase activity in tumors (**b**) were
302 examined 2 days after the last injection. Data are presented as mean ± SEM (N= 3 mice
303 per group). Statistical analysis was performed by one-way analysis of variance (ANOVA)
304 with Tukey post hoc test for comparison**.**

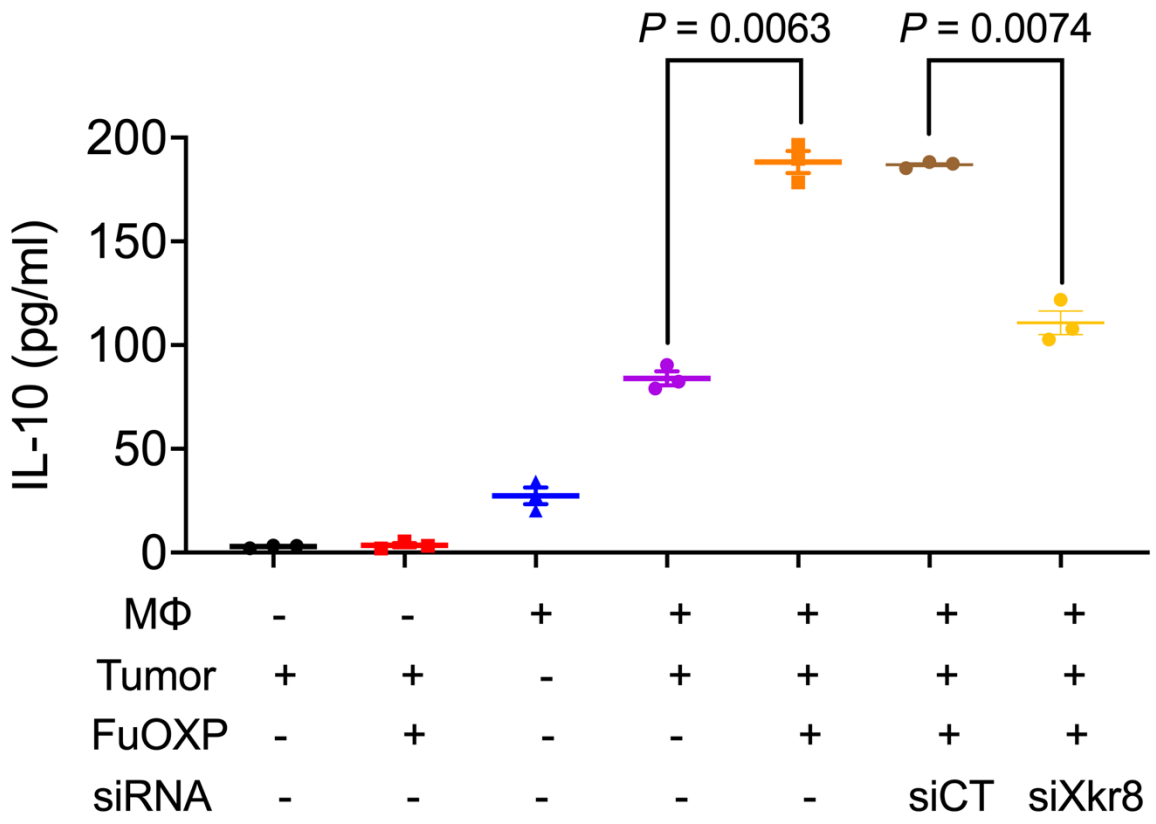

Suppl Fig. 18. IL-10 production by macrophages. CT26 tumor cells received various treatments as described in **Fig. 6a** and tumor cells were then co-cultured with resident peritoneal macrophages. Culture supernatants were collected after 24 h and IL-10 was quantified by a mouse IL-10 ELISA kit. Data are presented as mean ± SEM (N= 3). Statistical analysis was performed by one-way analysis of variance (ANOVA) with Tukey post hoc test for comparison.

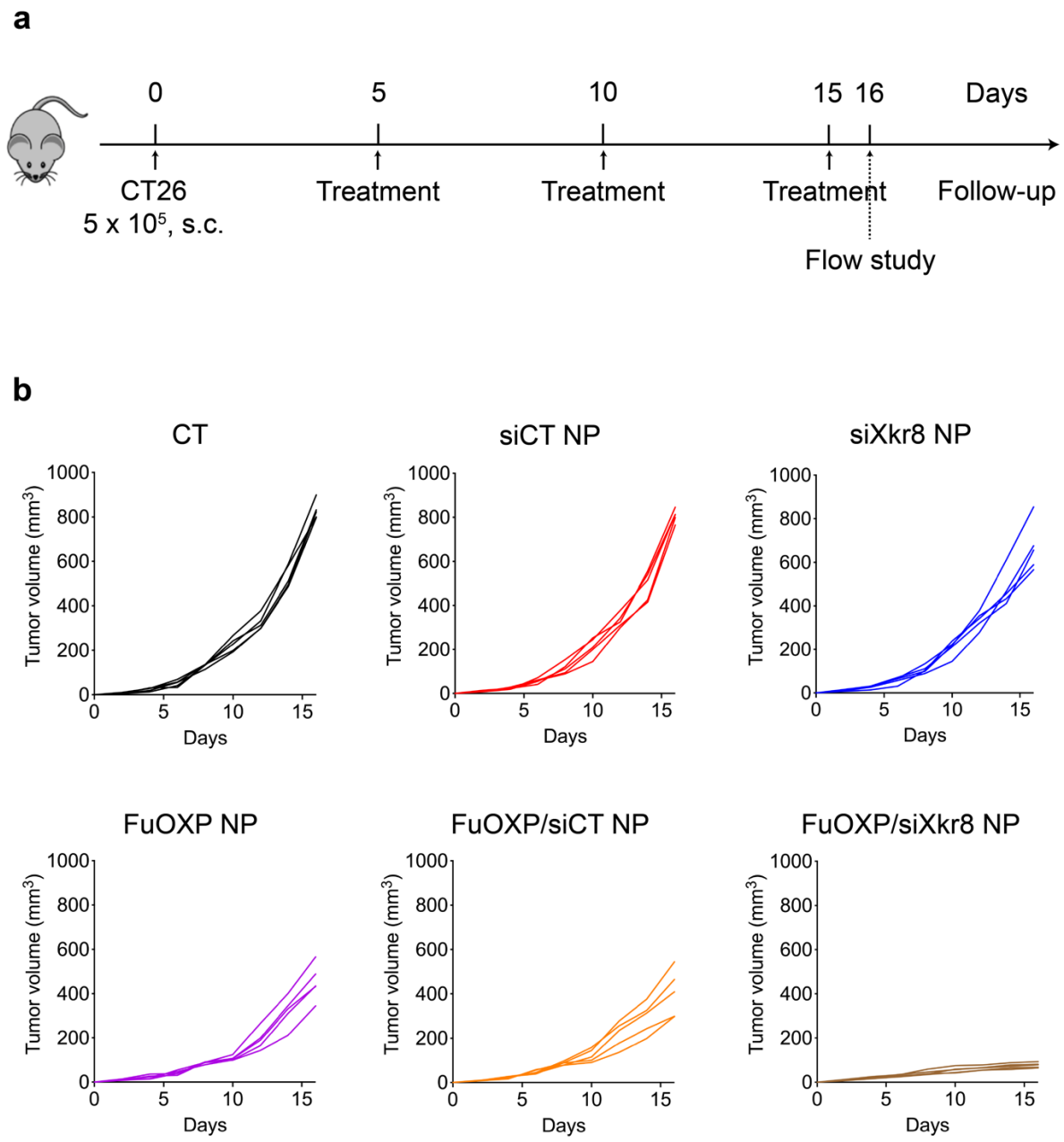

312

313 **Suppl Fig. 19. *In vivo* antitumor activity of FuOXP/siXkr8 NPs in CT26 model.** Mice
314 bearing CT26 tumors received various treatments once every 5 days for 3 times at a
315 siRNA dose of 1 mg/kg and FuOXP dose of 5 mg/kg. Tumor volumes were followed once
316 every 2 days. **a**: Treatment scheme; **b**: Individual tumor growth curves for mice bearing
317 CT26 tumors for **Fig. 6d**. Shown are representative data from 2 independent experiments
318 (n= 5).

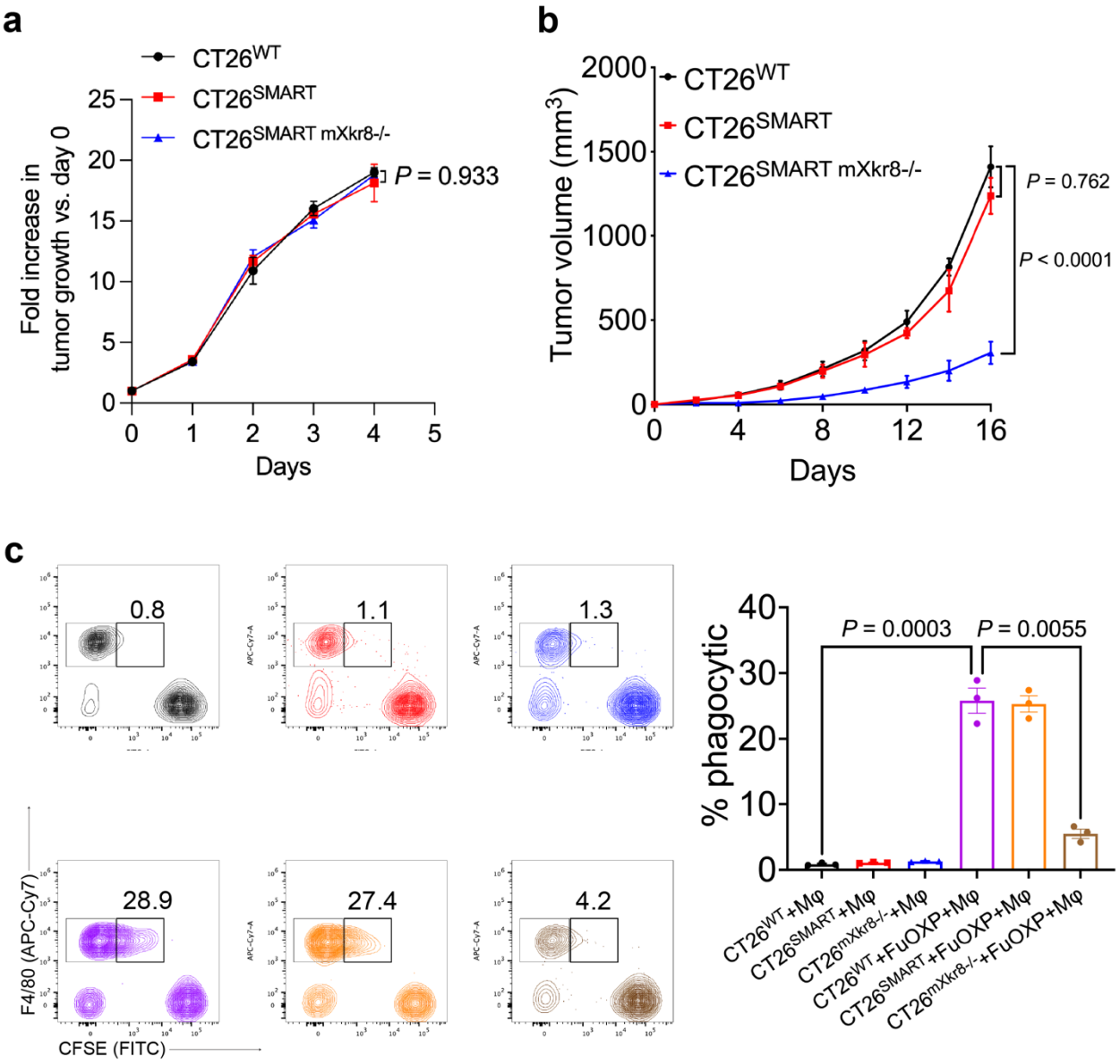

Suppl Fig. 20. Characterizations of CT26 subline with stable mXkr8 knockdown. a: MTT assay of cell proliferation of $CT26^{SMART\ mXkr8-/-}$, $CT26^{SMART}$ and $CT26^{WT}$ tumor cells at different timepoints. Data are presented as mean ± SEM (N= 6 replicates). **b**: $CT26^{SMART\ mXkr8-/-}$, $CT26^{SMART}$ and $CT26^{WT}$ tumor cells were s.c. inoculated into the right lower abdomen of BALB/c mice and the sizes of tumors were monitored once every 2 d. Data are presented as mean ± SEM (N= 8). **c**: $CT26^{SMART\ mXkr8-/-}$, $CT26^{SMART}$ and $CT26^{WT}$

326 tumor cells labelled with CFSE (FITC) were treated with DMSO or FuOXP (10 μM) for
327 24h followed by co-culture with resident peritoneal macrophages (stained with anti-F4/80
328 antibody). The numbers of $CFSE^+$ macrophages (APC-$Cy7^+$ & $F4/80^+$) were examined by
329 flow 1 h later. Data are presented as mean ± SEM (N= 3 replicates) and representative
330 of 2 independent experiments. Statistical analysis was performed by one-way analysis of
331 variance (ANOVA) with Tukey post hoc test for comparison.
332

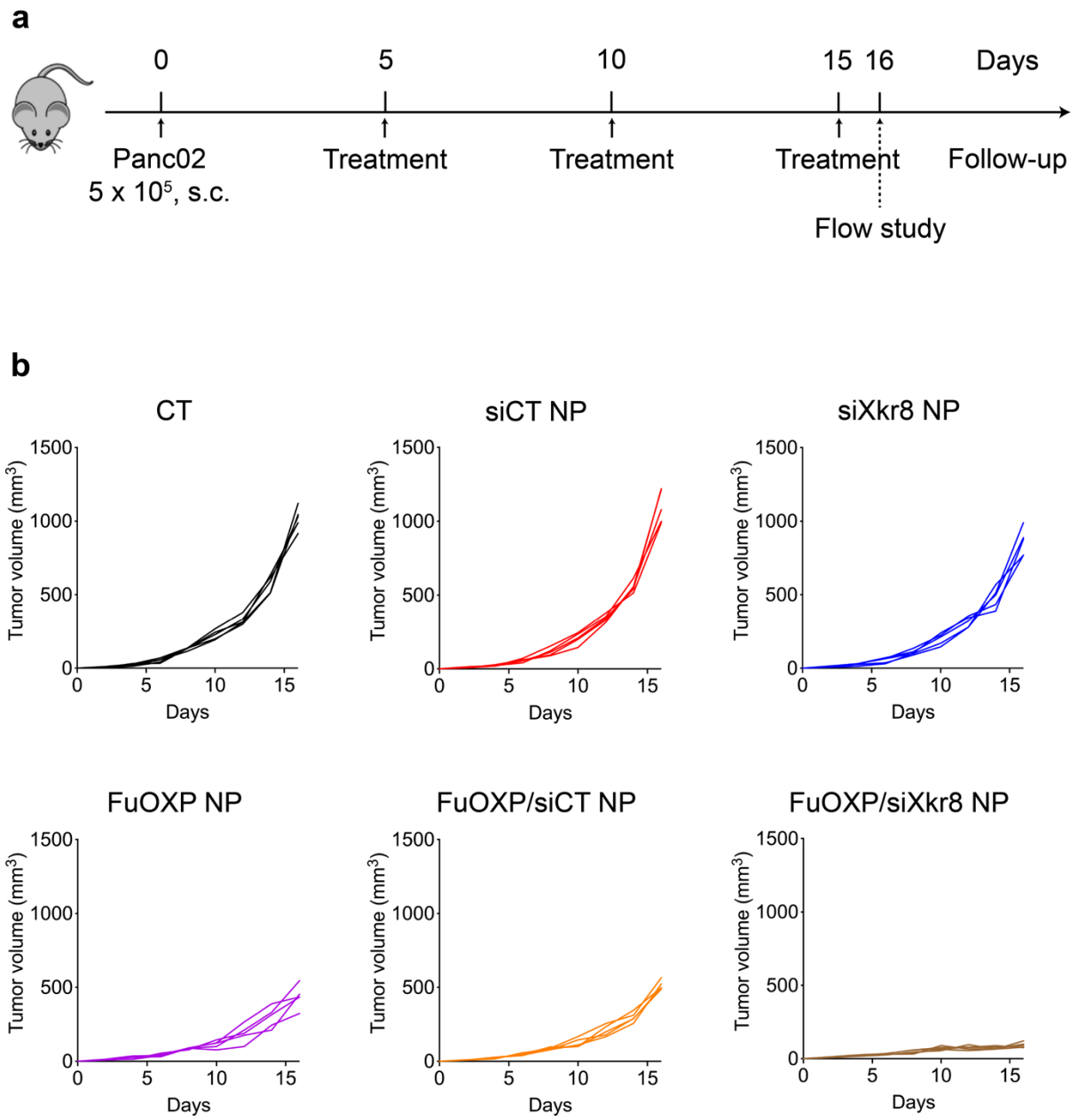

333

334 **Suppl Fig. 21. *In vivo* antitumor activity of FuOXP/siXkr8 NPs in Panc02 model.** Mice
335 bearing Panc02 tumors received various treatments once every 5 days for 3 times at a
336 siRNA dose of 1 mg/kg and FuOXP dose of 5 mg/kg. Tumor volumes were followed once
337 every 2 days. **a**: Treatment scheme; **b**: Individual tumor growth curves for mice bearing
338 Panc02 tumors for **Fig. 6e**. Shown are representative data of 2 independent experiments
339 (n= 5).

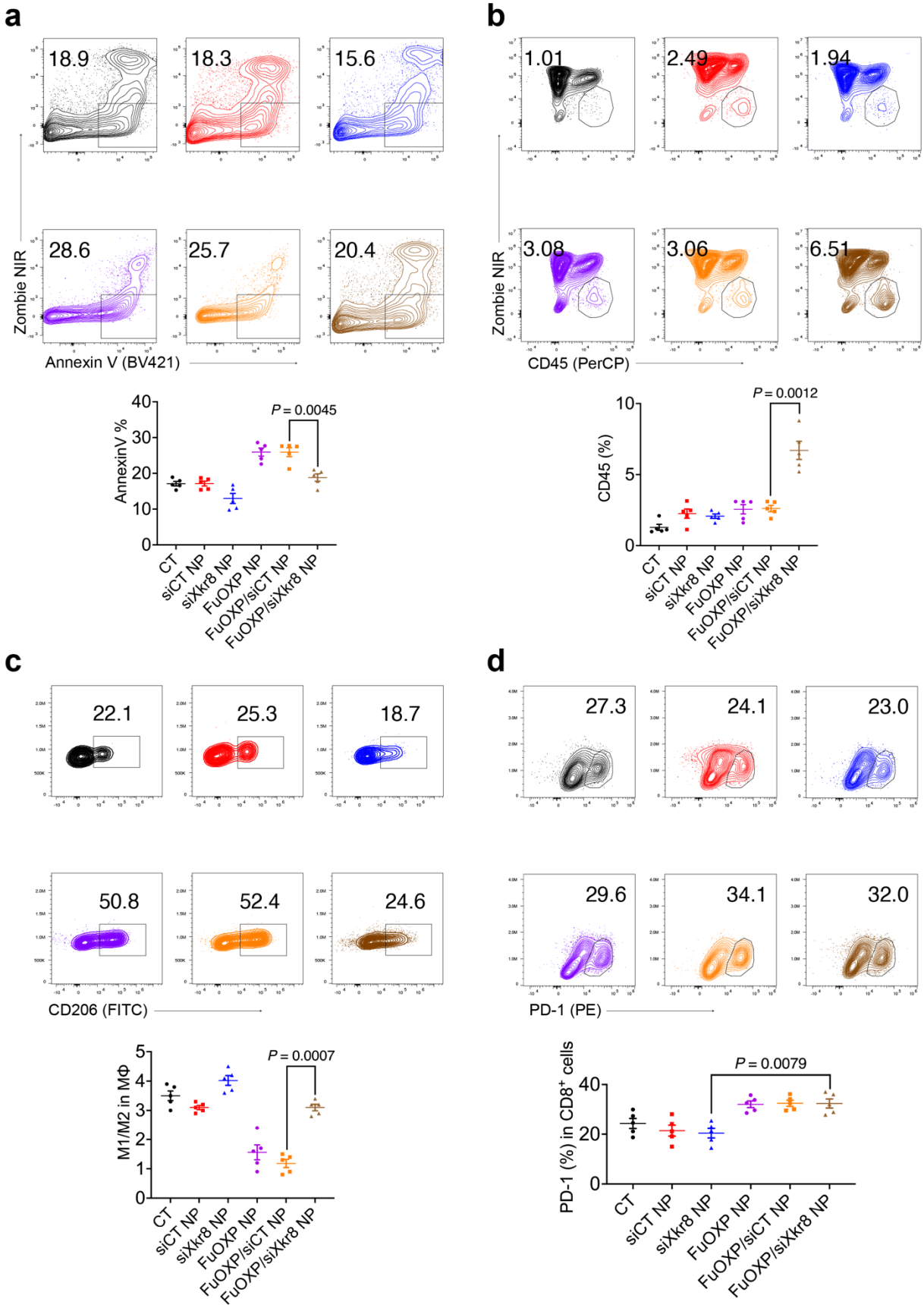
a
18.9
18.3
15.6
28.6
25.7
20.4
Zombie NIR
Annexin V (BV421)
AnnexinV %
P = 0.0045
b
1.01
2.49
1.94
3.08
3.06
6.51
Zombie NIR
CD45 (PerCP)
CD45 (%)
P = 0.0012
c
22.1
25.3
18.7
50.8
52.4
24.6
CD206 (FITC)
M1/M2 in MΦ
P = 0.0007
d
27.3
24.1
23.0
29.6
34.1
32.0
PD-1 (PE)
PD-1 (%) in CD8+ cells
P = 0.0079
CT
siCT NP
siXkr8 NP
FuOXP NP
FuOXP/siCT NP
FuOXP/siXkr8 NP

340

Suppl Fig. 22. Changes in tumor immune microenvironment following treatment with FuOXP/siXkr8-coloaded NPs. Mice bearing Panc02 tumors received various treatments once every 5 days for 3 times at a siRNA dose of 1 mg/kg and FuOXP dose of 5 mg/kg as described in **Fig. 6e**. Single cell suspensions were prepared at the completion of therapy study and subjected to various flow analyses including Annexin V^+ cells (**a**), $CD45^+$ cells (**b**), M1/M2-like ratios (**c**) and $PD1^+$ $CD8^+$ cells (**d**), respectively. Data are presented as mean ± SEM (N= 5 mice per group) and representative of 2 independent experiments. Statistical analysis was performed by one-way analysis of variance (ANOVA) with Tukey post hoc test for comparison.

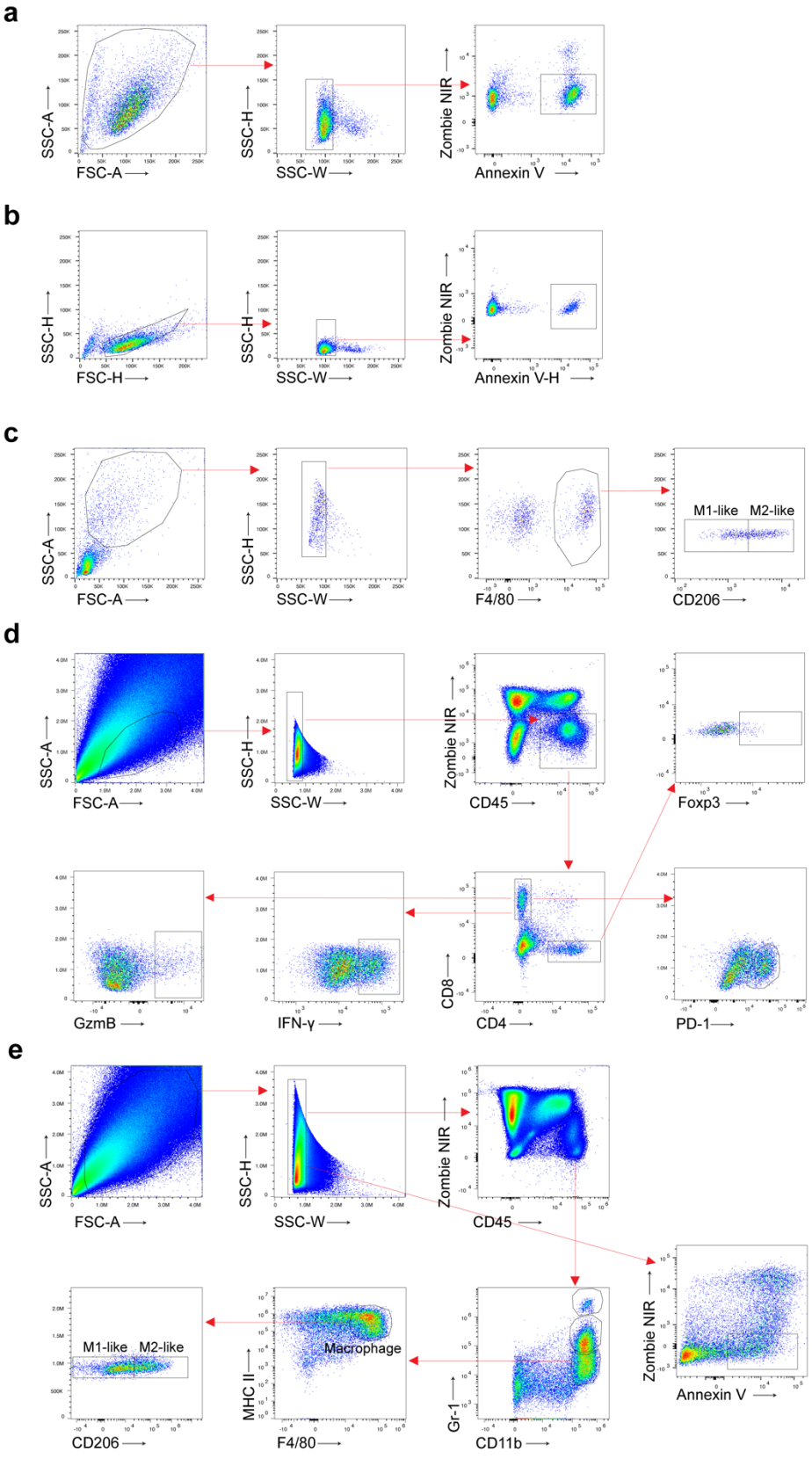
a
SSC-A
FSC-A
SSC-H
SSC-W
Zombie NIR
Annexin V
b
SSC-H
FSC-H
SSC-H
SSC-W
Zombie NIR
Annexin V-H
c
SSC-A
FSC-A
SSC-H
SSC-W
F4/80
CD206
M1-like
M2-like
d
SSC-A
FSC-A
SSC-H
SSC-W
Zombie NIR
CD45
Foxp3
GzmB
IFN-γ
CD8
CD4
PD-1
e
SSC-A
FSC-A
SSC-H
SSC-W
Zombie NIR
CD45
M1-like
M2-like
CD206
MHC II
F4/80
Macrophage
Gr-1
CD11b
Zombie NIR
Annexin V

350

Suppl Fig. 23. Gating strategies for different cell populations. Gating strategies for *in vitro* Annexin V^+ CT26 tumor cells (**a**), Annexin V^+ EVs (**b**), M1 and M2-like macrophages (**c**), *in vivo* $CD45^+$ cells, $CD4^+$ T cells, $CD8^+$ T cells, Treg cells, IFN-γ^+, $GzmB^+$ and PD-1^+ $CD8^+$ cells (**d**), Annexin V^+ CT26 tumor cells, M1 and M2-like macrophages (**e**) with Zombie NIR gating dead cells.

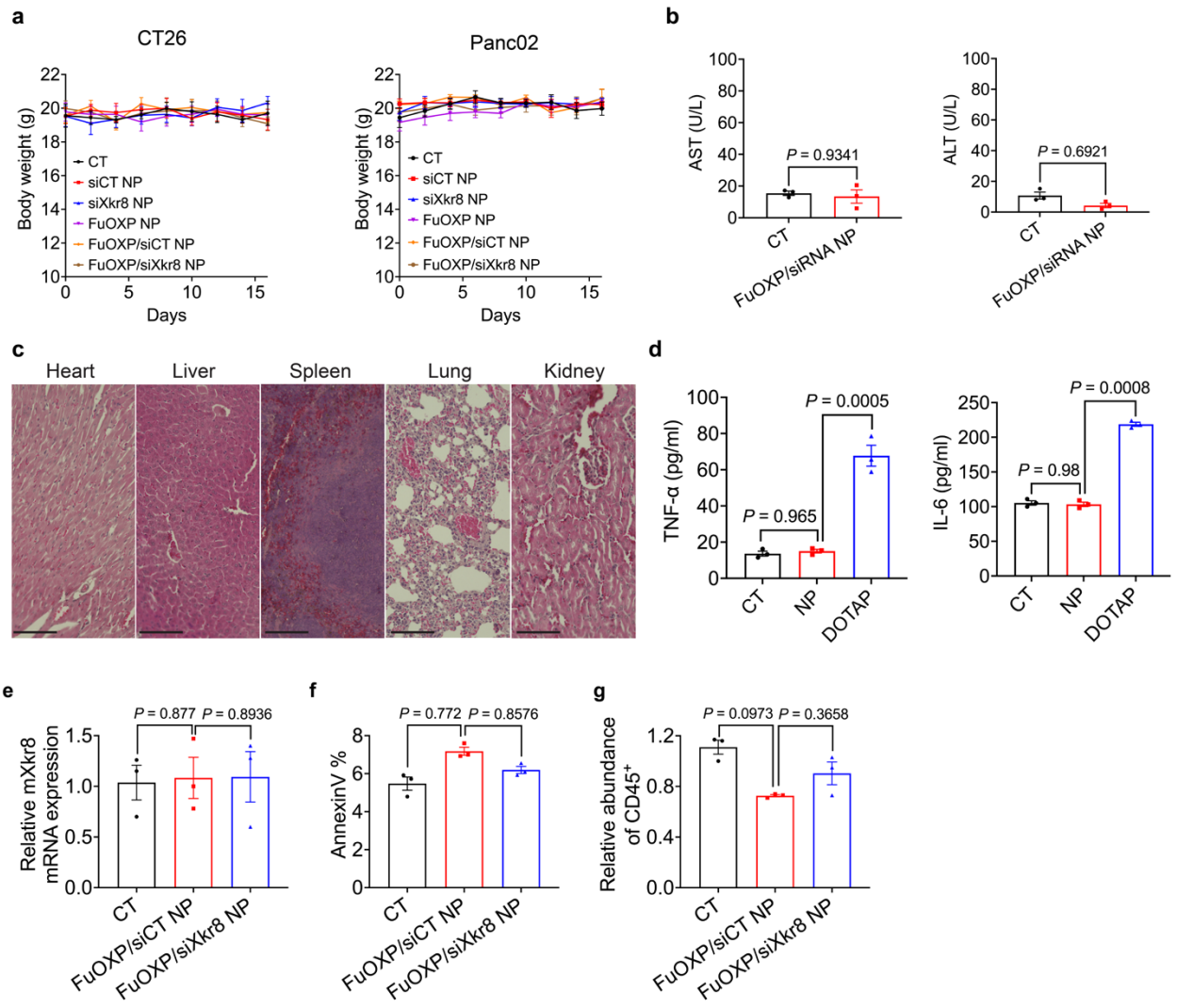

Suppl Fig. 24. Safety profiles of FuOXP/siXkr8-coloaded NPs. a: CT26 tumor-bearing mice received the treatments as described in **Fig. 6d**. Mouse weights were measured once every 2 days. Data are presented as mean ± SEM (N= 5 mice per group) and representative of 2 independent experiments. **b**: Serum levels of AST and ALT at the completion of the therapy study. Data are presented as mean ± SEM (N= 3 mice per group) and representative of 2 independent experiments. **c**: Histology of major organs in mice receiving different treatments as described in **Fig. 6d**. Scale bar, 50 μm. Shown are representative images from 2 independent experiments. **d**: Serum levels of TNF-α and IL-6 at 2 h following i.v. administration of siRNA PMBOP-CP NPs or siRNA complexed

with DOTAP liposomes (N/P, 10/1) at a siRNA dose of 1 mg/kg. Data are presented as mean ± SEM (N= 3 mice per group) and representative of 2 independent experiments. **e & f**: FuOXP NPs caused minimal changes in Xkr8 mRNA levels (**e**) and PS^+ cells (**f**) in liver. **g**: Minimal changes in $CD45^+$ cells in liver by FuOXP/siXkr8 NPs. Data (**e ~ g**) are presented as mean ± SEM (N= 3 mice per group) and representative of 2 independent experiments. Statistical analysis was performed by two-tailed Student's *t*-test for comparison in **b** and one-way analysis of variance (ANOVA) with Tukey post hoc test for comparison in **d**, **e**, **f** and **g.**

Inhibitor	Concentration
Chlorpromazine	25 µM (9 µg/mL)
Cytochalasin D	10 µM (5 µg/mL)
Filipin	3 µM (2 µg/mL)
Dynasore	80 µM (26 µg/mL)
Amiloride	100 µM (29 µg/mL)
MβCD	5 mM (7 mg/mL)

Suppl Table. 2. Various inhibitors of endocytic pathway

Supplementary References

1 Dobin, A. *et al.* STAR: ultrafast universal RNA-seq aligner. *Bioinformatics* **29**, 15-21, doi:10.1093/bioinformatics/bts635 (2013).

2 Trapnell, C. *et al.* Differential analysis of gene regulation at transcript resolution with RNA-seq. *Nat Biotechnol* **31**, 46-53, doi:10.1038/nbt.2450 (2013).

3 Tivol, W. F., Briegel, A. & Jensen, G. J. An improved cryogen for plunge freezing. *Microsc Microanal* **14**, 375-379, doi:10.1017/S1431927608080781 (2008).

4 Semple, S. C. *et al.* Rational design of cationic lipids for siRNA delivery. *Nat Biotechnol* **28**, 172-176, doi:10.1038/nbt.1602 (2010).

5 Belliveau, N. M. *et al.* Microfluidic Synthesis of Highly Potent Limit-size Lipid Nanoparticles for In Vivo Delivery of siRNA. *Mol Ther-Nucl Acids* **1**, doi:ARTN 37 10.1038/mtna.2012.28 (2012).

6 Brouckaert, G. *et al.* Phagocytosis of necrotic cells by macrophages is phosphatidylserine dependent and does not induce inflammatory cytokine production. *Mol Biol Cell* **15**, 1089-1100, doi:10.1091/mbc.e03-09-0668 (2004).

7 Ma, Z. *et al.* Cationic lipids enhance siRNA-mediated interferon response in mice. *Biochemical and Biophysical Research Communications* **330**, 755-759, doi:10.1016/j.bbrc.2005.03.041 (2005).